LAND SURFACE TEMPERATURE RETRIEVAL FROM DAYTIME AND NIGHTTIME LANDSAT 8 IMAGERY.

Bruno Rech [a]

[a] Department of Sanitary and Environmental Engineering, School of Technology, Federal University of Santa Catarina, Florianópolis, Brazil, b.rech@outlook.com.

Abstract. Land Surface Temperature (LST) represents Earth's surface temperature and is a parameter of great interest for various fields of study, such as hydrology and climate change. Whilst point observations are unable to account effectively for the spatial variability of LST, remote sensing techniques provide a robust assessment of the surface complexity regarding its temperature. In this sense, Landsat 8 satellite acquires thermal infrared data from the surface, and its higher spatial resolution is suitable for urban environment applications. Given the importance of LST for a diverse set of studies, this paper aimed to generate daytime and nighttime LST maps of Florianópolis metropolitan region. We assumed that Land Surface Emissivity (LSE) does not change significantly over scenes of the same area and temporally close (a few days) if no atmospheric precipitation occurs within the timespan between their acquisition dates. Therefore, LSE obtained for daytime could be combined with nighttime thermal infrared data for retrieving LST. This assumption was necessary since the shortwave data required for LSE estimation is not available for Landsat 8 nighttime imagery. The results showed a mean LST of 24.4 °C and 14.4 °C for day and night, respectively. For daytime, the higher temperatures were registered over built-up areas, while the lowest values represented vegetation. At night, the water bodies showed the highest LST, while the regions with lower values were also represented by vegetation. The applied methods have proven to be effective for retrieving LST from daytime and nighttime Landsat 8 scenes, and may provide LST data for the development of other studies.

Keywords. Land Surface Temperature, remote sensing, single-channel algorithm.

1. Introduction

Land Surface Temperature (LST) represents the surface temperature of the Earth and is an essential parameter for environmental monitoring, ecology, hydrology, climatic studies and many other fields [1]. Point field measurements of LST, however, are not good at representing its spatial variations.

In this sense, remote sensing techniques offer the possibility of retrieving LST from the entire globe with good spatial resolution. It provides a more robust assessment of the surface complexity, which is not possible through point measurements [2].

LST retrieval algorithms from satellite data can be categorized into single-channel, multi-channel and multi-angle methods. Single-channel algorithms use a single thermal infrared (TIR) band for estimating LST, while the others use two or more TIR bands at different wavelengths (multi-channel) or at different viewing angles (multi-angle). These techniques require Land Surface Emissivity (LSE) to be known a priori [2].

Although there are several satellites providing TIR data, Landsat and Aster (Advanced Spaceborne Thermal Emission and Reflection Radiometer) are the unique sources of thermal data applicable for the study of urban environments due to their higher spatial resolution [1].

As one of the most utilized satellites of the current time, Landsat 8 is operating since 2013 and is equipped with two onboard sensors: the Operational Land Imager (OLI) and the Thermal Infrared Sensor (TIRS). OLI produces 9 shortwave spectral bands at 30 m resolution (except for the panchromatic band, with 15 m), while TIRS produces two thermal bands: B10 (10.60 µm to 11.19 µm) and B11 (11.50 µm to 12.51 µm). The TIRS data is quantized to 12 bits and the originally 100 m spatial resolution is resampled to 30 m by the United States Geological Survey

(USGS). For quantitative analysis of TIRS data (e.g., LST retrieval), USGS discourages the use of B11 [3].

For some applications, it is also useful the assessment of LST at night [4]. According to USGS, nighttime acquisitions from Landsat 8 are made solely by special request [5]. Due to the absence of sunlight (i.e., the primary source of the radiation reflected by the surface and registered by Landsat 8 OLI), only the thermal bands from TIRS are useful from nighttime scenes. This characteristic poses an obstacle for the estimation of nighttime LST, since the visible and near infrared bands from OLI are required by LSE retrieval algorithms.

To by-pass this problem, [1] assumed that LSE does not change significantly over scenes of the same area and temporally close (a few days) if no atmospheric precipitation occurs within the timespan between their acquisition dates. Therefore, LSE obtained for daytime from OLI bands could be combined with nighttime TIRS data for retrieving LST.

Considering the aforementioned importance of surface temperature for a diverse range of applications, the present study aims to retrieve LST for daytime and nighttime over Florianópolis metropolitan region using Landsat 8 thermal data.

2. Research Methods

2.1 Study Area

The study area comprises the Florianópolis metropolitan region, located in the coast of the state of Santa Catarina, in Southern Brazil (figure 1). It includes the urban centres of the following municipalities: Águas Mornas, Antônio Carlos, Biguaçu, Florianópolis, Governador Celso Ramos, Palhoça, Santo Amaro da Imperatriz, São José and São Pedro de Alcântara. Together, these 9 municipalities sum up 1.25 million inhabitants [6].

Florianópolis is the main city of the region and the capital of the State of Santa Catarina, with approximately 575 thousand inhabitants. Between 1993 and 2013, its urbanized areas doubled [7], and this trend is also observed in the neighbouring cities.

Around 93% of Florianópolis territory is insular (Island of Santa Catarina). The study region is characterized by a mosaic of coastal plains and mountainous regions, with elevations ranging from sea level up to 1,000 m.

Köppen's climate classification for Florianópolis metropolitan region is Cfa, i.e., oceanic climate without dry season and with hot summer [8]. Mean annual air temperature and total precipitation are 21.1 °C and 1,766 mm, respectively [9].

2.2 Data

We selected two Landsat 8 images (Collection 2, Level 1), freely downloaded at USGS website (https://earthexplorer.usgs.gov/). The selection criteria took into consideration the acquisition timespan, the absence of cloud cover in the study region and the non-occurrence of rain between acquisition dates. Table 1 provides information about selected scenes.

Tab. 1 - Selected images information.

Type	Path	Row	Date
Daytime	220	079	20/04/2020
Nighttime	103	165	17/04/2020

Spectral bands were converted from digital number (DN) to radiance and reflectance values by [3]:

$$L_\lambda = M_L Q_{cal} + A_L \quad (1)$$

and

$$\rho_\lambda = \frac{M_\rho Q_{cal} + A_\rho}{\sin \theta_{se}} \quad (2)$$

where L_λ represents at sensor spectral radiance (W·m^{-2}·sr^{-1}·μm^{-1}), Q_{cal} is the Level 1 pixel value in DN, M_L and A_L are the respective radiance multiplicative and additive scaling factors, ρ_λ is the TOA planetary reflectance, θ_{se} is the local sun elevation angle and M_ρ and A_ρ are the respective reflectance multiplicative and additive scaling factors.

The meteorological data was downloaded from the Brazilian National Institute of Meteorology database (https://bdmep.inmet.gov.br/) for the weather station A806, located at coordinates 27°36'00" S and 48°37'12" W.

2.3 Land Surface Emissivity Retrieval

For LSE calculation, a NDVI-based method from [10] was adopted considering Landsat 8 TIRS band 10:

$$\varepsilon = \begin{cases} a_1 + \sum_{j=2}^{7} a_j \rho_j, & NDVI < 0.2 \\ \varepsilon_v P_v + \varepsilon_s (1 - P_v) + d\varepsilon, & 0.2 \le NDVI \le 0.5 \\ \varepsilon_v + d\varepsilon, & NDVI > 0.5 \end{cases} \quad (3)$$

where ε is LSE, ρ_j is the apparent reflectance of OLI band j, ε_s and ε_v are the respective soil and vegetation emissivities (adopted as 0.971 and 0.982), P_v is the fractional vegetation cover, $d\varepsilon$ is a term accounting for the cavity effect and $a_1 - a_7$ are given coefficients (for further details, see [10]).

2.4 Land Surface Temperature Retrieval

LST was derived from TOA radiance of Landsat 8 TIRS B10 using the Practical Single-Channel (PSC) algorithm proposed by [11] as given:

$$T_s = \frac{c_2/\lambda}{\ln\left[\frac{c_1}{\lambda^5 B(T_s)} + 1\right]} \quad (4)$$

where T_s is the LST (K), coefficients c_1 = 1.19104×10^8 W·μm^4·m^{-2}·sr^{-1}, c_2 = 1.43877×10^4 μm·K, λ is the effective wavelength (10.904 μm for L8 TIRS band 10) and $B(T_s)$ is the blackbody radiance from land surface (W·m^{-2}·sr^{-1}·μm^{-1}).

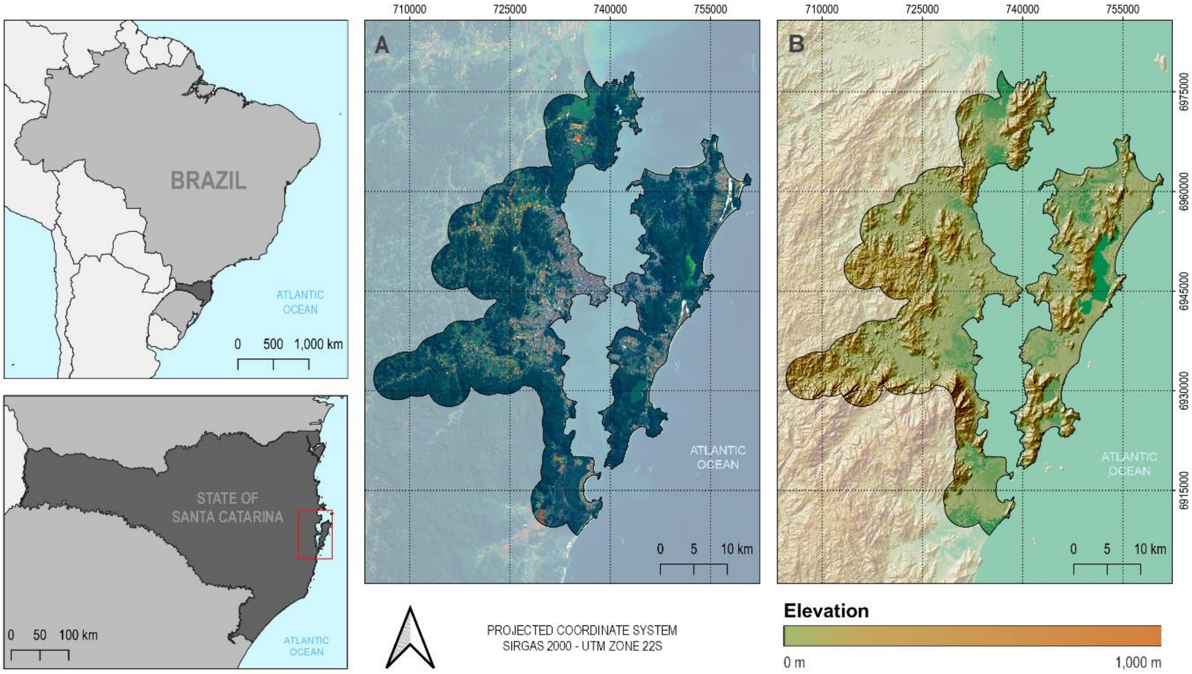

Fig. 1 - Location of the study area presenting a) the selected daytime scene in true colour composition and b) the elevation map.

Blackbody radiance was calculated by [11]:

$$B(T_s) = b_0 + b_1 w + (b_2 + b_3 w + b_4 w^2)\frac{1}{\varepsilon} + (b_5 + b_6 w + b_7 w^2)\frac{L_\lambda}{\varepsilon} \quad (5)$$

where $b_0 - b_7$ are coefficients (see [11]), w is the atmospheric water content (g·cm^{-2}), ε is the emissivity and L_λ is at sensor spectral radiance of Landsat 8 TIRS band 10 (W·m^{-2}·sr^{-1}·µm^{-1}).

Atmospheric water content was derived from atmospheric data of weather station using the equations from [12, 13]:

$$w = 0.098 \times RH \times 6.1121 \times (1 + 7.2 \times 10^{-4} + [3.2 \times 10^{-6} + 5.9 \times 10^{-10} T_a^2]P) \times \exp\left(\frac{\left[18.729 - \frac{T_a}{227.3}\right]T_a}{T_a + 257.87}\right) \quad (6)$$

where RH is the relative humidity, T_a is near-surface air temperature (°C) and P is the atmospheric pressure (mbar).

3. Results and Discussion

The application of the algorithm produced LST values over the study area, covering approximately 1.46 million pixels (spatial resolution of 30 m) on each band. Table 2 summarises the values of LST retrieved from both daytime and nighttime scenes.

As can be observed in figure 2, the highest values of daytime LST are associated with built-up areas, bare soil and dunes. The maximum temperature (38.4 °C), however, was registered over a sanitary landfill. Vegetated areas and water showed similar temperatures. The lowest values represent vegetation over portions of the terrain oriented due west and south, which receives less solar radiation.

Tab. 2 - Summary of LST estimates for day and night.

Statistic	Daytime (°C)	Nighttime (°C)
Minimum	17.4	4.1
1st quartile	22.8	13.0
Median	24.0	14.4
Mean	24.4	14.4
3rd quartile	25.9	15.8
Maximum	38.4	22.1

For nighttime, mean temperature decreased 10 °C compared with daytime LST. In this case, the highest values were registered over water bodies, followed by built-up areas. Unlike daytime LST, surface temperature at night does not show a clear pattern. For instance, some densely-vegetated regions presented values quite similar to built-up areas.

At night, most of the colder places are located in the mountainous regions at the continent. Minimum LST was registered over a shopping mall. The rural areas (with sparse human occupation and with presence of agriculture) showed not only lower LST compared with daytime, but also compared with nighttime LST of other land cover classes.

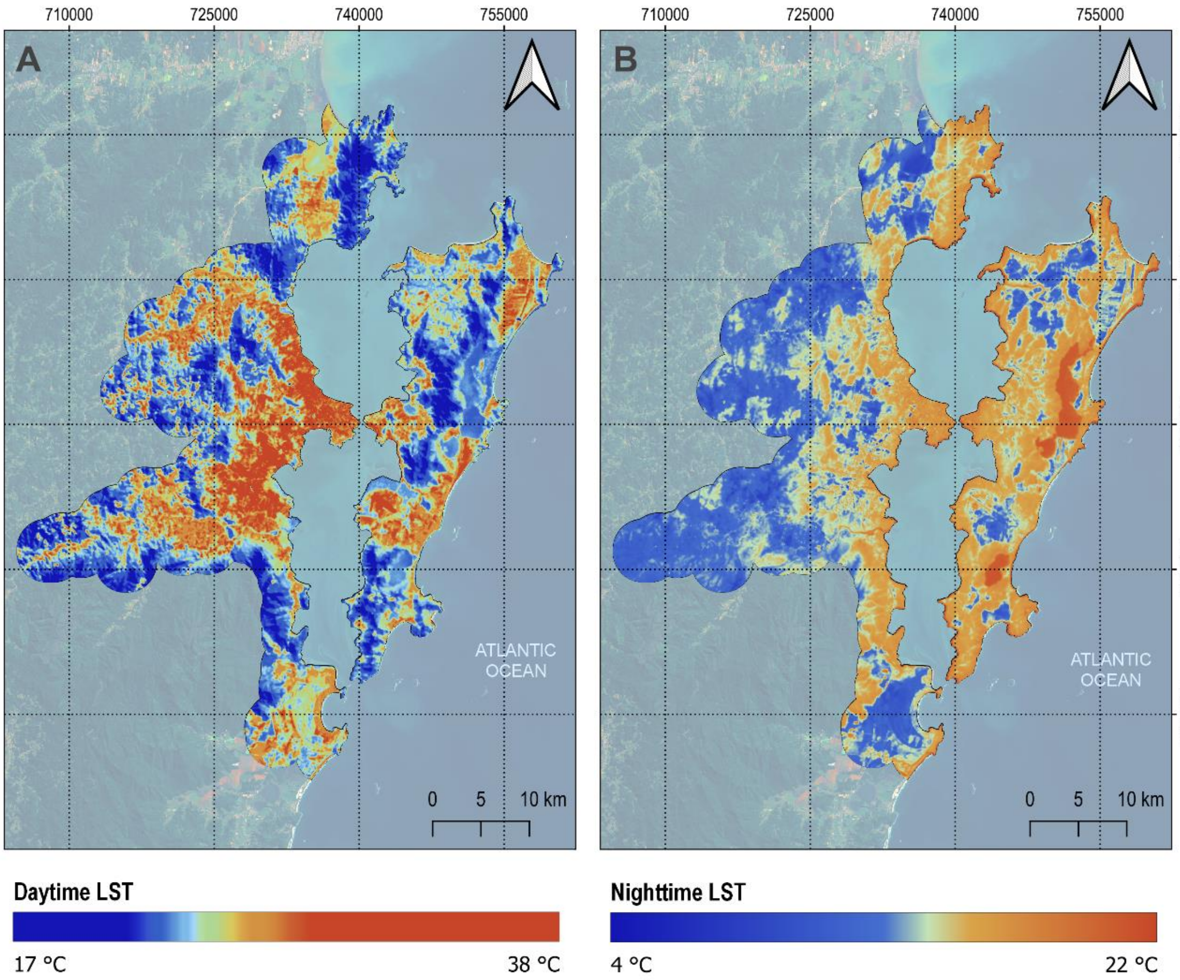

Fig. 2 – Results of LST retrieval for a) daytime and b) nighttime.

It's possible to observe that at daytime, LST values are mainly dictated by solar radiation. In surfaces with low water availability, such as built-up areas, most of the absorbed solar radiation is converted into sensible heat (i.e., increases temperature). Over vegetation and water bodies, the solar radiation is the source of energy for evapotranspiration, which converts the absorbed energy into latent heat. This mechanism explains why urban areas are hotter than vegetation and water during the day.

For the nighttime, LST depends mainly on the capacity of the surface in retaining heat. Water has a great specific heat capacity, which is the reason behind the higher values of LST over water bodies. However, there isn't a clear pattern for built-up and vegetation areas. These regions are possibly influenced by the direction of the winds and also for the configuration of surface (e.g., more densely-occupied urban areas can retain more heat than sparsely-occupied areas).

4. Conclusions

The applied methods have proven to be effective for retrieving LST from daytime and nighttime Landsat 8 scenes. In the study area, the general means were of 24.4 °C and 14.4 °C for day and night, respectively.

The low availability of images is challenging for nighttime LST estimations, since most of them don't meet the assumption of absence of precipitation or are covered by clouds. Furthermore, LST is a seldom-measured parameter in Brazil, which turns the validation of remote sensing estimates with field observations a rather difficult task.

LST presents great variability over the surface and its behaviour differs from day to night. For this reason, further analyses may be carried out for characterizing LST variations over different land cover classes at daytime and nighttime.

5. Acknowledgement

I would like to acknowledge: INCBAC Institute for the opportunity of developing my scientific skills; professors Jan Komárek and Tomáš Klouček for this fruitful academic cooperation, and; my colleagues Rodrigo Nehara and Tiago Mello for the shared knowledge, the dedication on the development of our study, the moments of fun and the friendship.

6. References

[1] Sekertekin A, Bonafoni S. Sensitivity Analysis and Validation of Daytime and Nighttime Land Surface Temperature Retrievals from Landsat 8 Using Different Algorithms and Emissivity Models. *Remote Sensing*. 2020; 12(17):2776.

[2] Li ZL, Tang BH, Wu H, Ren H, Yan G, Wan Z, et al. Satellite-derived land surface temperature: Current status and perspectives. *Remote Sens Environ*. 2013; 131:14–37.

[3] USGS. *Landsat 8 (L8) Data Users Handbook*. 5th ed. Sioux Falls: USGS; 2019.

[4] Abdullah H, Omar D k., Polat N, Bilgili AV, Sharef SH. A comparison between day and night land surface temperatures using acquired satellite thermal infrared data in a winter wheat field. *Remote Sens Appl*. 2020; 19.

[5] USGS. *Landsat Acquisitions* [Internet]. USGS. 2022. Available from: https://www.usgs.gov/landsat-missions/landsat-acquisitions

[6] IBGE. *Censo 2022* [Internet]. IBGE. 2023. Available from: https://www.ibge.gov.br/estatisticas/sociais/populacao/22827-censo-demografico-2022.html?edicao=35938&t=resultados

[7] Lopes M das N, Dalpiaz FL, Rech B, Teixeira JD, Ribeiro ISS, Magri D, et al. Trends in aquatic ecology research associated with urbanization evolution during three decades in Santa Catarina Island/SC. *Acta Limnologica Brasiliensia*. 2020; 32:e205.

[8] Alvares CA, Stape JL, Sentelhas PC, de Moraes Gonçalves JL, Sparovek G. Köppen's climate classification map for Brazil. *Meteorologische Zeitschrift*. 2013; 22(6):711–28.

[9] INMET. *Normais Climatológicas do Brasil 1991-2020*. Brasília; 2022. Available from: https://portal.inmet.gov.br/normais#

[10] Li S, Jiang GM. Land Surface Temperature Retrieval from Landsat-8 Data with the Generalized Split-Window Algorithm. *IEEE Access*. 2018; 6:18149–62.

[11] Wang M, Zhang Z, Hu T, Liu X. A Practical Single-Channel Algorithm for Land Surface Temperature Retrieval: Application to Landsat Series Data. *Journal of Geophysical Research: Atmospheres*. 2019; 124(1):299–316.

[12] Buck AL. New Equations for Computing Vapor Pressure and Enhancement Factor. *Journal of Applied Meteorology*. 1981; 20(12):1527–32.

[13] Yu X, Guo X, Wu Z. Land Surface Temperature Retrieval from Landsat 8 TIRS – Comparison between Radiative Transfer Equation-Based Method, Split Window Algorithm and Single Channel Method. *Remote Sensing*. 2014; 6(10):9829–52.